Communication

Mesostructured Selenides with Cubic MCM-48 Type Symmetry: Large Framework Elasticity and Uncommon Resiliency to Strong Acids

Pantelis N. Trikalitis, Nan Ding, Christos Malliakas, Simon J. L. Billinge, and Mercouri G. Kanatzidis

J. Am. Chem. Soc., **2004**, 126 (47), 15326-15327• DOI: 10.1021/ja044954r • Publication Date (Web): 05 November 2004

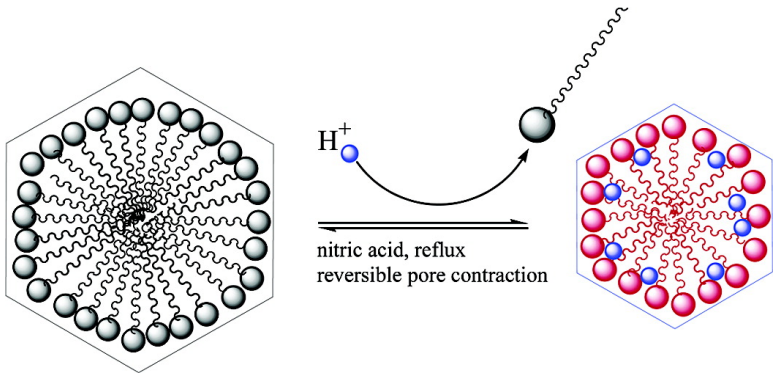

More About This Article

Additional resources and features associated with this article are available within the HTML version:

- Supporting Information
- Links to the 1 articles that cite this article, as of the time of this article download
- Access to high resolution figures
- Links to articles and content related to this article
- Copyright permission to reproduce figures and/or text from this article

View the Full Text HTML

J|A|C|S
COMMUNICATIONS

Published on Web 11/05/2004

Mesostructured Selenides with Cubic MCM-48 Type Symmetry: Large Framework Elasticity and Uncommon Resiliency to Strong Acids

Pantelis N. Trikalitis,[†] Nan Ding,[†] Christos Malliakas,[†] Simon J. L. Billinge,[‡] and Mercouri G. Kanatzidis*,[†]

Departments of Chemistry and Physics, Michigan State University, East Lansing, Michigan 48824

Received August 20, 2004; E-mail: kanatzid@cem.msu.edu

Recently, the surfactant templating route has been extended to non-oxidic porous mesostructured materials based on metal−chalcogenido anions such as $[MQ_4]^{4-}$, $[M_2Q_6]^{4-}$, and $[M_4Q_{10}]^{4-}$ (M = Ge, Sn; Q = S, Se, Te) and various linking metal ions.[1−3] Under proper experimental conditions, materials with remarkably high hexagonal or cubic symmetry have been synthesized.[1,2] These represent non-oxidic analogues of the well-known mesoporous silica materials (MCM, SBA, MSU, etc.)[4] and are of interest for potential multiple functionality imparted by the inorganic framework (optical, semiconducting, metallic) in combination with nanoscale periodicity and porosity. The pores in these materials are occupied by surfactant molecules used as templates. Although the presence of guest molecules in the pores is desirable, it is also important to establish accessibility of the pore system. Thus far, attempts to remove the template from mesostructured chalcogenides by thermal decomposition led to collapse of the inorganic framework.[2] Another method to remove the template and access the pore space would be ion-exchange. Typically, in the case of silicates the as-synthesized materials are treated in an acidic solution where the cationic long-chain organic molecules are replaced by protons.

Ion-exchange properties of the pore space in mesostructured chalcogenides have been demonstrated in the cubic *c*-C_{20}PyPtSnSe (*Ia*-3*d*),[5] where the long-chain surfactant $C_{20}Py^+$ [5] are replaced with shorter-chain-length $C_{12}Py^+$ molecules. The Pt/Sn/Se framework forms by the reaction of $[Sn_2Se_6]^{4-}$ and square planar Pt^{2+} centers and adopts a cubic double-gyroid structure similar to that of MCM-48.[6] This motif has open channels running in three different directions.

Here we report the surprising result that *c*-C_nPyPtSnSe, which can grow in micrometer-sized single-crystalline faceted cubosome morphology, can ion-exchange their surfactant molecules with H^+ from strong acids without decomposition. This is remarkable behavior, given that metal chalcogenido anionic frameworks generally decompose in strong acids. During this H^+-exchange process, the framework actually contracts while maintaining its single-crystalline morphology, structural integrity, and composition. It then expands when the larger surfactant molecules are exchanged back in. Such "breathing" behavior is unusual and implies that the Pt/Sn/Se framework in these solids is both robust and elastic. This is in sharp contrast to the silicate counterparts, which exhibit definite framework rigidity under the same conditions.[7] The acid-exchanged materials, denoted as *c*-H_C_{20}PyPtSnSe, diffract X-rays as well as their pristine counterparts.[8]

XRD patterns from the pristine *c*-C_{20}PyPtSnSe and those of the acid-treated products are shown in Figure 1. The XRD patterns (Figure 1a−c) show a strong peak followed by a weak reflection at the low-angle region $2° < 2\theta < 6°$, typical of mesostructured materials. The two peaks correspond to (211) and (220) reflections

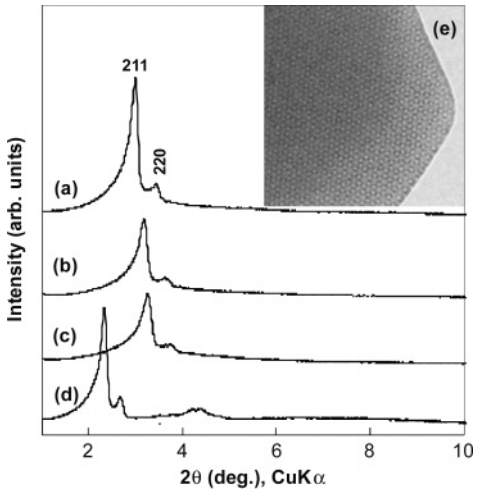

Figure 1. XRD patterns of (a) *c*-H_C_{20}PyPtSnSe (HCl), (b) *c*-H_C_{20}PyPtSnSe (H_2SO_4), (c) *c*-H_C_{20}PyPtSnSe (HNO_3), and (d) pristine *c*-C_{20}PyPtSnSe material; (e) TEM image of the pore system in *c*-C_{20}PyPtSnSe, looking down the [111] axis.

of a cubic cell with *Ia*-3*d* space group symmetry. These reflections are clearly shifted to higher 2θ angles compared to those reflections from the as-synthesized material (Figure 1d), betraying a topotactic ion-exchange process and a spectacular contraction of the unit cell that exceeds 55% of the original volume (see Table 1). The pore symmetry shown in the transmission electron microscopy (TEM) image of Figure 1e is preserved, as discussed below. This contraction comes from the uniform contraction of the pores and is due to the replacement of the large alkyl pyridinium molecules by the small protons. A volume change of this magnitude is, to the best of our knowledge, unprecedented in any mesoporous material. The process can be reversed when *c*-H_C_{20}PyPtSnSe is treated with excess C_{20}PyBr, as all reflections move to lower angles and the unit cell expands.

The acid treatment is in fact an ion-exchange process, as the surfactant content is significantly reduced.[9] Compared to the pristine material (43.53 wt % $C_{20}Py^+$), the corresponding values for the HCl-, H_2SO_4-, and HNO_3-treated solids are 18.16, 18.25, and 14.81 wt %, respectively (see Table 1). This is more that 60 wt % of the surfactant cations exchanged with protons. It is also amazing that the *c*-C_{20}PyPtSnSe materials retain their structure and mesoscopic long-range pore order after such an enormous cell volume change. Furthermore, the exceptional stability of *c*-C_nPyPtSnSe in HNO_3 and the absence of oxidative degradation is astonishing, considering that these materials are metal selenides. One could expect attack of the metal selenide framework by protons and formation of volatile H_2Se.

Scanning electron microscopy (SEM) images show cubosome particles, similar to those in the parent *c*-C_{20}PyPtSnSe (see

[†] Department of Chemistry.
[‡] Department of Physics.

10.1021/ja044954r CCC: $27.50

Table 1. Elemental Analyses, Powder XRD Data, Unit Cell Parameters, and Colors for Cubic Mesostructured Platinum Tin Selenides

			powder XRD data				
sample	% C, H, N	Pt:Sn:Se[a]	d_{211}/Å	d_{220}/Å	unit cell constant,[b] a (Å)	vol. contraction,[c] (%)	color
HCl_C_{20}PyPtSnSe	14.46, 2.80, 0.90	0.97:2:5.85	29.9	25.9	73	54.4	black
H_2SO_4_C_{20}PyPtSnSe	15.06, 2.42, 0.77	1.0:2:5.76	28.0	24.5	69	61.8	black
HNO_3_C_{20}PyPtSnSe	12.16, 2.01, 0.64	1.0:2:5.57	27.4	23.9	67	64.6	black
c-C_{20}PyPtSnSe	36.14, 5.61, 1.78	0.96:2:5.78	38.6	33.3	95		dark brown

[a] EDS data normalized with Sn atom ratio. [b] Calculated on the basis of (211) reflection using the formula $a = d_{hkl}(h^2 + k^2 + l^2)^{1/2}$. [c] Compared to the pristine material.

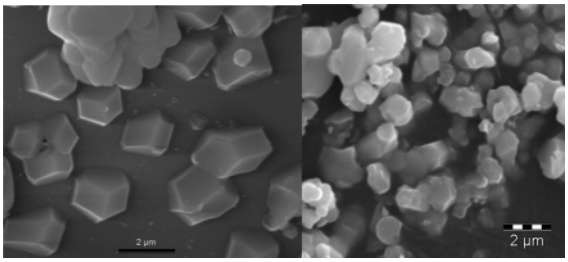

Figure 2. SEM images of (left) as-synthesized *c*-C_{20}PyPtSnSe and (right) H_2SO_4_C_{20}PyPtSnSe particles showing contracted grain size yet preserved cubosome morphology.

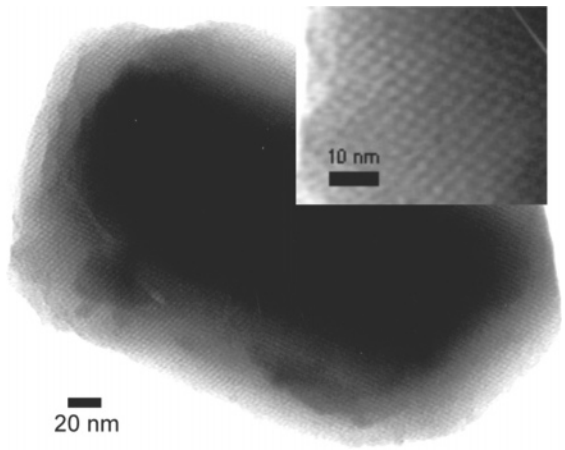

Figure 3. TEM images of *c*-H_C_{20}PyPtSnSe (H_2SO_4) single particle. Inset: pore structure consistent with the cubic *Ia*-3*d* symmetry, [110] direction.

Figure 2). The symmetry, pore organization, and morphology of the cubosome C_{20}PyPtSnSe particles persist after acid treatment and are readily observable by SEM and TEM. Figure 3 shows a typical TEM image of a single grain of *c*-H_C_{20}PyPtSnSe, viewed down the [110] axis, showing a uniform pore order. The pore system is clearly seen in the inset. The estimated pore−pore separation and unit cell dimensions are in agreement with those determined by XRD.

The local structure of the Pt/Sn/Se framework is intact in the acid-exchanged materials, as indicated by X-ray diffuse scattering and pair distribution function (PDF) analysis.[10] Figure 4 shows PDF plots as a function of distance for pristine and HCl-treated *c*-C_{20}PyPtSnSe. It is apparent that the overall pair-distance distribution in the two materials is nearly identical, with the peaks at 2.5 Å corresponding to Pt−Se and Sn−Se nearest-neighbor bonding, whereas those at 3.7 Å are due to second-nearest-neighbor distances, such as Pt···Sn and Se···Se. Beyond 7 Å, atomic pair correlations are not observed, confirming the aperiodic nature of the inorganic wall system.

In conclusion, the cubic mesostructured *c*-C_{20}PyPtSnSe materials are exceptionally stable in strong acids, exchanging a large fraction of the surfactants with H^+. The structural robustness is a significant

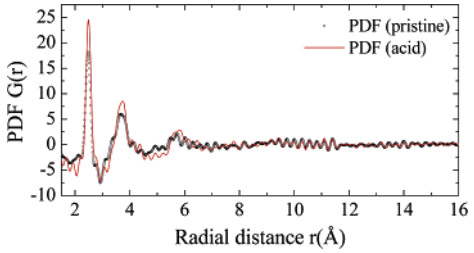

Figure 4. Reduced pair distribution function $G(r)$ of pristine (black curve) and acid-exchanged (red curve) *c*-C_{20}PyPtSnSe, plotted against distance r (synchrotron 120 keV radiation).

if not unexpected property, given that these are metal chalcogenides. Unlike the stiff tetrahedral-based silicate frameworks, the Pt/Sn/Se framework appears to be highly flexible as it contracts/expands without loss of local structural order or nanoperiodicity. This could be due to the presence of more flexible square planar Pt^{2+} centers in the structure. The strength and flexibility of the Pt−Sn−Se network, coupled with the accessibility of its pores and its unique ability to undergo very large reversible pore volume changes, suggests that these systems are amenable to a wide variety of postsynthetic manipulations.

Acknowledgment. Support from NSF Grant CHE-0211029, Chemistry Research Group, is acknowledged.

Supporting Information Available: XRD patterns of HNO_3_C_{20}-PyPtSnSe material and the corresponding solid; table of elemental analyses, powder XRD data and colors. This material is available free of charge via the Internet at http://pubs.acs.org.

References

(1) MacLachlan, M. J.; Coombs, N.; Ozin, G. A. *Nature* **1999**, *397*, 681−684.
(2) (a) Trikalitis, P. N.; Rangan, K. K.; Bakas, T.; Kanatzidis, M. G. *Nature* **2001**, *410*, 671. (b) Trikalitis, P. N.; Rangan, K. K.; Kanatzidis, M. G. *J. Am. Chem. Soc.* **2002**, *124*, 2604−2613.
(3) Riley, A. E.; Tolbert, S. H. *J. Am. Chem. Soc.* **2003**, *125*, 4551−4559.
(4) (a) Kresge, C. T.; Leonowicz, M. E.; Roth, W. J.; Vartuli, J. C.; Beck, J. S. *Nature* **1992**, 359, 710−712. (b) Schuth, F. *Angew. Chem., Int. Ed.* **2003**, *42*, 3604.
(5) Trikalitis, P. N.; Rangan, K. K.; Bakas, T.; Kanatzidis, M. G. *J. Am. Chem. Soc.* **2002**, *124*, 12255 ($C_{20}Py^+$= $C_{20}H_{41}$-NC_5H_5 cation).
(6) Alfredsson, V.; Anderson, M. W. *Chem Mater*. **1996**, *8*, 1141−1146.
(7) Hitz, S.; Prins, R. *J. Catal.* **1997**, *168*, 194−206.
(8) High-quality *c*-C_{20}PyPtSnSe with cubic *Ia*-3*d* symmetry was synthesized following method reported elsewhere.[5] Proton exchange was carried out in concentrated ethanolic solutions of HCl, H_2SO_4, and HNO_3. In a typical experiment, 0.2 g of *c*-C_{20}PyPtSnSe was placed in a 50 mL round-bottom flask, and 30 mL of ethanol and 10 mL of 2 M solution of acid were added. The mixture was refluxed overnight. A black solid was obtained by filtration, washed with copious amounts of ethanol, and dried in air.
(9) The elemental composition was determined by energy-dispersive microprobe analysis (SEM/EDS) and elemental C, H, and N (see Table 1). No S or Cl was detected. In addition, no compositional changes were observed, as judged by the Pt/Sn/Se ratio in all acid-treated samples, and there was no evidence of inorganic elements leaching into solution.
(10) Billinge, S. J. L.; Kanatzidis, M. G. *Chem. Commun.* **2004**, 749−760.

JA044954R